Chapter 3. Epitaxial Growth and Processing of Compound Semiconductors

Academic and Research Staff

Professor Leslie A. Kolodziejski, Dr. Gale S. Petrich, Dr. Jay N. Damask

Graduate Students

Jody L. House, Elisabeth M. Koontz, Kuo-Yi Lim, Jeremy M. Milikow, Steven G. Patterson, Sean C. Warnick

Technical and Support Staff

Olga M. Arnold, Angela R. Mickunas

3.1 Introduction

The emphasis of this research program is the epitaxial growth and processing of III-V compound semiconductors. The epitaxial growth of the heterostructures is performed in the chemical beam epitaxy laboratory. The laboratory consists of two gaseous source epitaxy reactors interconnected to several smaller chambers which are used for sample introduction and *in-situ* surface analysis. Such a multichamber epitaxy system allows heterostructures to be fabricated within a continuous ultrahigh vacuum environment. The III-V gas source molecular beam epitaxy (GSMBE) reactor is equipped with (1) solid elemental sources of Ga, In, Al, Si and Be, (2) gaseous hydride sources of arsenic and phosphorus, (3) an atomic hydrogen source to remove the sample's native surface oxide prior to growth and (4) an *in situ* spectroscopic ellipsometer to characterize the epilayer during growth.

In the following sections, the status of the various III-V-based projects will be discussed. The III-V GSMBE system is utilized for (1) the development of (In,Ga)(As,P)-based optical devices for optical networks, (2) the fabrication of one-, two- and three-dimensional photonic bandgap crystals, and (3) the fabrication of bandgap-engineered distributed Bragg reflectors for vertical cavity surface emitting lasers.

3.2 Development of Semiconductor Optical Devices for All-Optical Communication Networks

Sponsors

MIT Lincoln Laboratory

U.S. Air Force - Office of Scientific Research
Grant F49620-96-1-0126

Project Staff

Professor Leslie A. Kolodziejski, Professor Erich P. Ippen, Professor Henry I. Smith, Professor James G. Fujimoto, Professor Hermann A. Haus, Dr. Mark S. Goorsky,[1] Dr. Gale S. Petrich, Dr. Katherine L. Hall, Dr. Günter Steinmeyer, Dr. Jay N. Damask, Elisabeth M. Koontz, Jeremy M. Milikow, Igor P. Bilinsky, David J. Jones, Erik R. Thoen, Thomas E. Murphy, M. Jalal Khan, Michael H. Lim, K.M. Matney,[2] Greg D. U'Ren[3]

With the next generation of all-optical networks being designed for operation at speeds of 100 Gbits/sec and higher, compact, efficient semiconductor-based optical devices are clearly in demand. In these high bit-rate networks, low-loss wavelength-selective routing devices and ultrafast (femtosecond) optical pulse sources are required.

1 Department of Material Science and Engineering, University of California, Los Angeles, California.

2 Ibid.

3 Ibid.

Waveguide-coupled Bragg-resonant filters[4] provide a compact means of achieving high-density wavelength-selective routing. The functionality of the planar version of these filters[5] is contingent upon the ability to preserve the as-fabricated rectangular-patterned Bragg gratings during the gas source molecular beam epitaxial overgrowth. Mass transport-induced degradation of the rectangular-grating profile during the epitaxial overgrowth results in the inability to selectively route the desired wavelength.[6]

Rectangular-patterned gratings, similar in dimension to those required by the Bragg-resonant filters, have been fabricated in both InP and InGaAsP. An *in-situ* low-temperature atomic hydrogen-assisted oxide removal technique has been employed to preserve the rectangular grating profile[7] as seen in Figure 1. The atomic hydrogen-assisted cleaning process is performed at 200°C, well below the temperature required to thermally desorb the native oxide from the sample's surface (~ 470°C). Thus, the overgrowth can be nucleated immediately upon arrival at the growth temperature (480°C), severely inhibiting the degradation of the grating profile via mass transport effects.

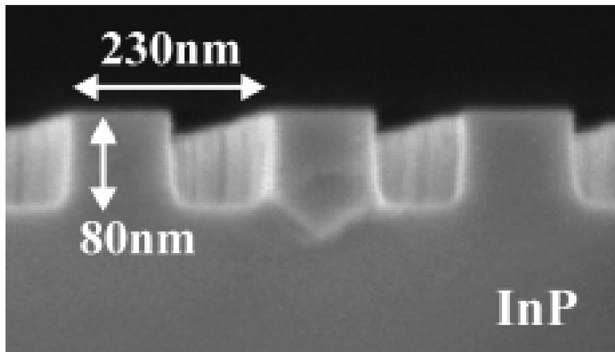

Figure 1. Scanning electron micrograph of an InP rectangular-patterned grating following the low temperature atomic hydrogen-assisted oxide removal process.

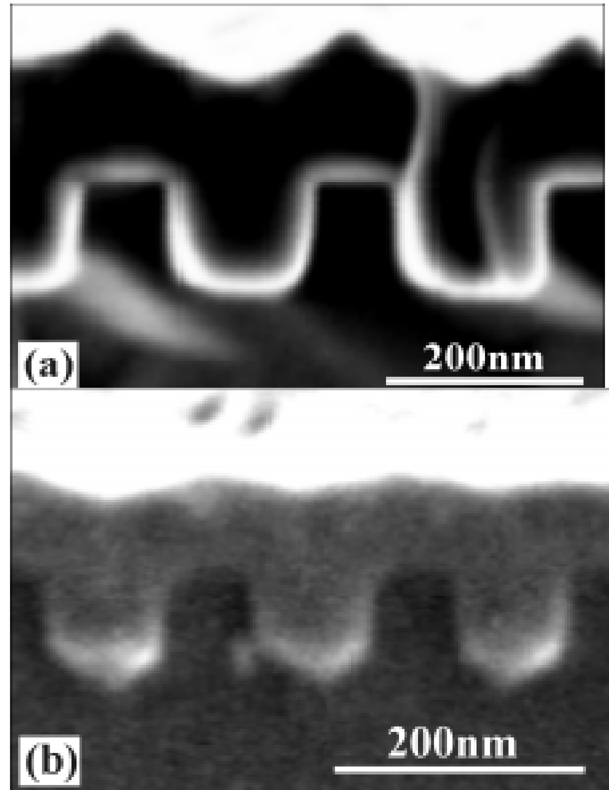

Figure 2. (a) Scanning electron micrograph of 200 nm of InGaAs deposited on a hydrogen-cleaned InP grating. (b) Scanning electron micrograph of 200 nm of InGaAs deposited on a thermally-cleaned InP grating; the as-fabricated rectangular grating shows signs of mass transport-induced profile degradation.

Figure 2 depicts a scanning electron micrograph of an overgrown hydrogen-cleaned InP grating (Figure 2a) and a thermally-cleaned InP grating (Figure 2b). The hydrogen-cleaned grating appears to be intact, while the thermally-cleaned grating has experienced profile degradation in the form of rounded grating teeth and filled-in grating trenches.

4 H.A. Haus and Y. Lai, "Narrow-Band Distributed Feedback Reflector Design," *J. Lightwave Technol.* 9(6): 754-60 (1991); H.A. Haus and Y. Lai, "Narrow-Band Optical Channel-Dropping Filter," *J. Lightwave Technol.* 10(1): 57-62 (1992).

5 J.N. Damask, "Practical Design of Side-Coupled Quarter-Wave Shifted Distributed-Bragg Resonant Filters," *J. Lightwave Technol.* 14(5): 812-21 (1996).

6 J.N. Damask, private communication.

7 E.M. Koontz, M.H. Lim, V.V. Wong, G.S. Petrich, L.A. Kolodziejski, H.I. Smith, M.S. Goorsky, and K.M. Matney, "Overgrowth of InGaAsP Materials on Rectangular-patterned Gratings Using GSMBE," *Proceedings of the Ninth International Conference on InP and Related Materials,* Hyannis, Massachusetts, May 11-15, 1997.

Triple-axis x-ray diffractometry (TAD) has been used to provide a nondestructive, high-resolution analysis of the overgrown gratings. A (004) TAD reciprocal space map of InGaAsP deposited on an InP grating is shown in Figure 3. The zeroth order satellite reflection is similar to a double crystal x-ray scan and reveals the high quality of the overgrown InGaAsP. The existence of periodic satellite fringes confirms the presence of a periodic modulation within the overgrown structure. Separation of the satellite fringes (Δ) is related to the period of the grating[8] and corresponds to an as-fabricated period of 230 nm. The vertical continuity of the satellite reflections (along q_{004}) represents the retention of the rectangular grating profile.[9] The presence of the ±2nd order satellite reflections (not expected for rectangular grating profiles having equal trench and tooth widths[10]) suggests the presence of strain within the grating region.[11] The appearance of the ±2nd order satellite reflections cannot be attributed to a mass transport-induced change in the InP grating profile from rectangular to gaussian since the higher order satellite reflections are of significant intensity.[12] (224) TAD reciprocal space maps confirm that strain is present within the grating region, and is orthorhomically distorting the crystal.[13] In other words, two of the three lattice components are strained to differing amounts, while the third lattice component is left unstrained. The magnitude of the strain is on the order of 10^{-3} and is expected to have a minimal effect on the optical characteristics of the Bragg-resonant filters.[14]

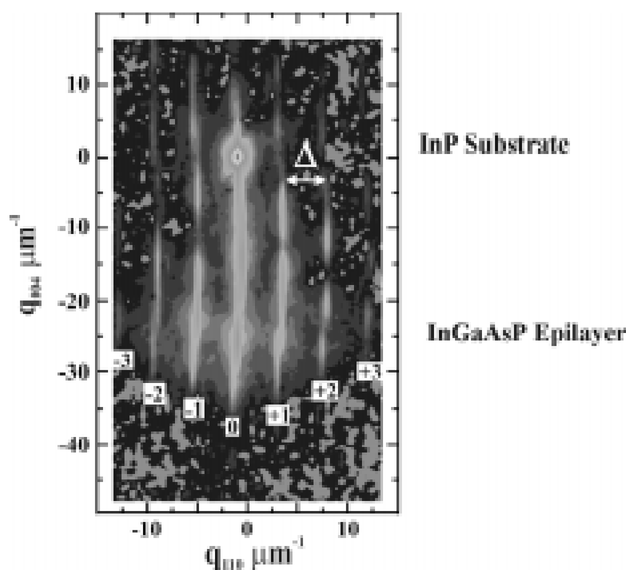

Figure 3. A (004) triple axis x-ray diffraction-generated reciprocal space map of 200 nm of $In_{0.93}Ga_{0.07}As_{0.23}P_{0.77}$ deposited on a hydrogen-cleaned InP grating.

Currently, passive modelocking is the most practical method of generating ultrashort (femtosecond) pulses in lasers. The shortest pulses achieved thus far, 6.5 fsec, are from a Ti:sapphire laser implementing a semiconductor saturable absorber mirror to initiate modelocking.[15] Ti:sapphire lasers, however, operate at a wavelength (0.75 µm) significantly below that required for efficient transmission over standard communications optical fiber (1.3 µm or 1.55 µm), upon which the all-optical communication systems are based. Various chromium-based solid-state lasers have been successfully modelocked at wavelengths within the 1.5 µm regime,[16] with the passive

8 A.T. Macrander and S.E.G. Slusky, "X-ray Diffraction from Corrugated Crystalline Surfaces and Interfaces," *Appl. Phys. Lett.* 56(5):443-45 (1990).

9 P. van der Sluis, "High Resolution X-ray Diffraction of One- and Two-dimensional Periodic Surface Gratings," *J. Phys. III France* 4: 1639-47 (1994).

10 Ibid.

11 E.M. Koontz, M.H. Lim, V.V. Wong, G.S. Petrich, L.A. Kolodziejski, H.I. Smith, K.M. Matney, G.D. U'Ren, and M.S. Goorsky, "Preservation of Rectangular-patterned InP Gratings Overgrown by Gas Source Molecular Beam Epitaxy," *Appl. Phys. Lett.* 71(10): 1400-02 (1997).

12 G.D. U'Ren, M.S. Goorsky, E.M. Koontz, M.H. Lim, G.S. Petrich, L.A. Kolodziejski, V.V. Wong, H.I. Smith, K.M. Matney, and M. Wormington, "Analysis of Lattice Distortions in High Quality InGaAsP Epitaxial Overgrowth of Rectangular-patterned InP Gratings," *J. Vac. Sci. Technol. B.*, forthcoming.

13 Ibid.

14 Ibid.

15 I.D. Jung, F.X. Kartner, N. Matuschek, D. Sutter, F. Morier-Genoud, U. Keller, V. Scheuer, M. Tilsch, T. Tschudi, and R. Szipocs, "Self-starting 6.5 fs Pulses from a KLM Ti:sapphire Laser," *Proceedings of the Conference on Lasers and Electro-Optics,* (Washington, DC: Optical Society of America, 1997), 11: 35 (1997).

modelocking devices being saturable Bragg reflectors (SBRs). Also successfully modelocked (at $\lambda \sim$ 1.53 μm) via an SBR is a linear erbium/ytterbium co-doped fiber laser cavity.[17] Modelocked fiber lasers offer a number of advantages over other ultrafast sources, such as their compactness and ability to be pumped with telecommunications-certified low-power laser diodes, and a wavelength of operation centered at the erbium-doped fiber gain peak of 1.55 μm.

An SBR consists of a saturable absorber (quantum wells within a half-wave layer or a bulk-like epilayer) integrated with a highly reflective mirror, a distributed Bragg reflector (DBR). By epitaxially depositing the saturable absorber directly on the mirror via gas source molecular beam epitaxy, additional fabrication steps (i.e., thinning or removing the substrate beneath the saturable absorber and using index matching epoxy to attach a saturable absorber to a commercial mirror) are avoided. In addition, by selecting the reflectivity of the DBR, the SBR can then be used as either a high reflector or an output coupler in the laser cavity.

The current SBR structures contain either two or four InGaAs quantum wells positioned 15 nm from the top of, or centered within, the InP half-wave layer. The DBR contains 22 pairs of quarter-wave AlAs/GaAs layers, resulting in a reflectivity spectrum centered at 1.55 μm. Of concern is the large lattice mismatch between the InP half-wave layer and the GaAs-based DBR. The use of a half-wave InP layer has two purposes: it does not harm the reflectivity spectrum of the DBR, yet simultaneously provides a buffer between the lattice-mismatched InP/GaAs interface and the InGaAs quantum well absorber.

The transmission spectrum from a 22-pair DBR and the photoluminescence spectrum of an SBR containing two InGaAs quantum wells centered within the InP half-wave layer are shown in Figure 4. Additional analysis performed on the SBRs include pump-probe measurements (changes in frequency and reflectivity with respect to time and wavelength) and phase change measurements (changes in the phase with respect to time and wavelength). Two SBRs, both with two InGaAs quantum wells positioned 15 nm from the top of the InP half-wave layer, have successfully modelocked a Cr^{4+}:YAG laser. Devices are currently being fabricated for implementation in erbium-doped fiber ring and sigma laser cavities as well as linear fiber cavities containing an erbium/ytterbium co-doped amplifier, all of which integrate easily with all-optical fiber networks.

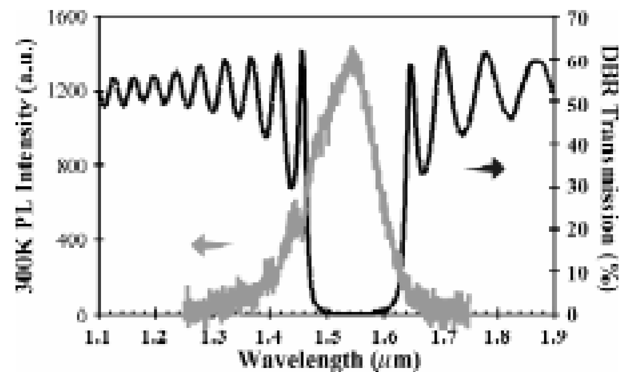

Figure 4. Transmission spectrum of a 22-pair AlAs/GaAs distributed Bragg reflector (DBR) and photoluminescence spectra of a saturable Bragg reflector consisting of the 22-pair DBR and two InGaAs quantum wells centered within an InP half-wave layer.

3.2.1 Publications

Koontz, E.M., M.H. Lim, V.V. Wong, G.S. Petrich, L.A. Kolodziejski, H.I. Smith, K.M. Matney, G.D. U'Ren, and M.S. Goorsky. "Preservation of Rectangular-patterned InP Gratings Overgrown by Gas Source Molecular Beam Epitaxy." *Appl. Phys. Lett.* 71(10): 1400-02 (1997).

Koontz, E.M., M. H. Lim, V.V. Wong G.S. Petrich, L.A. Kolodziejski, H.I. Smith, M.S. Goorsky, and K.M. Matney. "Overgrowth of InGaAsP Materials on Rectangular-patterned Gratings Using GSMBE." *IEEE Proceeedings of the Ninth International Conference on InP and Related Materials,* Hyannis, Massachusetts, May 11-15, 1997.

16 B.C. Collings, J.B. Stark, S. Tsuda, W.H. Knox, J.E. Cunningham, W.Y. Jan, R. Pathak, and K. Bergman, "Saturable Bragg Reflector Self-starting Passive Mode Locking of a Cr^{4+}:YAG Laser Pumped with a Diode-pumped Nd:YVO_4 Laser," *Opt. Lett.* 21(15): 1171-73 (1996); M.J. Hayduk, S.T. Johns, M.F. Krol, C.R. Pollock, and R.P. Leavitt, "Broadly Tunable Saturable Absorber Mode-locked Cr^{4+}:YAG Femtosecond Laser," *Proceedings of the IEEE Lasers and Electro-Optics Society Annual Meeting,* (Piscataway, N.J.: IEEE, 1996), pp. 54-55.

17 B.C. Collings, K. Bergman, S. Tsuda, and W.H. Knox, "Femtosecond Short Cavity 2.5 GHz Fiber Laser Harmonically Mode-locked by a Saturable Bragg Reflector with Low Temporal Jitter," *Proceedings of the Conference on Lasers and Electro-Optics* (Washington, D.C.: Optical Society of America, 1997); 11: 343-44 (1997).

U'Ren, G.D., M.S. Goorsky, E.M. Koontz, M.H. Lim, G.S. Petrich, L.A. Kolodziejski, V.V. Wong, H.I. Smith, K.M. Matney, and M. Wormington. "Analysis of Lattice Distortions in High Quality InGaAsP Epitaxial Overgrowth of Rectangular-patterned InP Gratings." Sixteenth North American Conference on Molecular Beam Epitaxy, Ann Arbor, Michigan, October 5-8, 1997; *J. Vac. Sci. Tech. B.* Forthcoming.

3.3 Photonic Bandgap Structures

Sponsor

National Science Foundation
Grant DMR 94-00334

Project Staff

Professor John D. Joannopoulos, Professor Leslie A. Kolodziejski, Professor Erich P. Ippen, Professor Henry I. Smith, Dr. Gale S. Petrich, Dr. Pierre R. Villeneuve, Dr. Shanhui Fan, Dr. Günter Steinmeyer, Kuo-Yi Lim, Daniel J. Ripin

This project represents the combined effort of the research groups led by Professors John D. Joannopoulos, Leslie A. Kolodziejski, Erich P. Ippen, and Henry I. Smith. Professor Joannopoulos' research group designs the structures and theoretically calculates the optical properties. Professor Kolodziejski's group fabricates various devices exhibiting photonic band structures in one-, two-, and three-dimensions using III-V compound semiconductor technologies. Professor Smith's group provides the expertise in nanoscale fabrication. Finally, the devices are optically characterized by Professor Ippen's research group. The complexity of the design, fabrication and characterization of these structures necessitates a strong interaction between the various research groups.

A photonic crystal is a periodic dielectric structure that prohibits the propagation of photons within a certain range of frequencies in all directions. This forbidden band of frequencies translates into a photonic bandgap (PBG) analogous to an electronic bandgap in a semiconductor crystal. A defect state can be introduced in the photonic bandgap when the dielectric periodicity of a photonic crystal is broken by the selective removal or addition of dielectric material. This defect results in the spatial localization of the defect mode into a volume of approximately one cubic wavelength, yielding a low modal volume, high-quality factor resonant microcavity. The realization of such a microcavity holds the promise of vastly enhancing the performance of optoelectronic devices through its effect on spontaneous emission.

3.3.1 One-Dimensional Photonic Bandgap Devices: Monorail and Air-Bridge Microcavities

The one-dimensional photonic bandgap devices that are being investigated at MIT are referred to as monorail and air-bridge microcavity devices. In the monorail microcavity, the photonic crystal consists of a GaAs waveguide with an array of holes etched through the waveguide. The holes are spaced periodically and a defect is created by introducing additional separation in the middle of the array. The photonic crystal resides on a layer of aluminum oxide (Al_xO_y) which has a much lower refractive index than GaAs (n = 1.61 versus n = 3.3). In the air-bridge microcavity, the photonic crystal is suspended in air (n = 1.0), resulting in a higher index contrast between the crystal and its surroundings. The devices are designed to operate at the technologically important wavelength of 1.55 μm. Consequently, the photonic crystal has a width of 0.5 μm and a thickness of 0.2 μm. The hole diameter, separation, and defect width are 0.2 μm, 0.4 μm, and 0.6 μm respectively. Both the monorail and air-bridge microcavities have waveguides coupled into and out of the devices to facilitate the optical characterization of these devices.

The fabrication process for the devices utilize a heterostructure of $GaAs/Al_{0.9}Ga_{0.1}As$ grown by gas source molecular beam epitaxy. Subsequently, a series of plasma-enhanced chemical vapor deposition, electron-beam lithography, reactive ion etch, photolithography and wet etch processing steps are employed to fabricate the final devices. The samples are then thinned from 400 μm to 150 μm before a final cleave is performed to create mirror-smooth facets at the waveguide ends for optical coupling. Both the monorail and air-bridge microcavity structures have been successfully fabricated and are currently being characterized. Figure 5 shows a scanning electron micrograph of a completed one-dimensional photonic bandgap device.

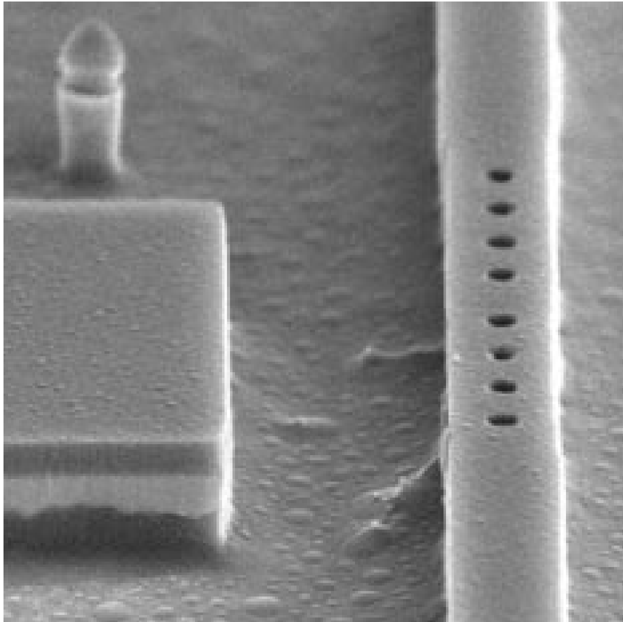

Figure 5. A micrograph of a PBG monorail structure with a GaAs waveguide. The width and thickness of the bridge are 0.5 µm and 0.2 µm, respectively. The diameter and separation of the holes are 0.4 µm and 0.6 µm, respectively.

The one-dimensional photonic crystal results in the confinement of light of a particular wavelength along the direction of the waveguide. At the same time, the light is also confined in the other two directions by total internal reflection. The wavelength of light being confined in the microcavity is determined by the dimensions and separation of the holes in the photonic crystal. The combination of the high-index contrast of the system and the presence of the photonic crystal results in a high-Q, low-modal volume microcavity. Such a microcavity can effectively alter the spontaneous emission rate of an active region located in the microcavity.

3.3.2 Two-Dimensional Photonic Bandgap Device: Enhancing the Extraction Efficiency of a Light Emitting Diode

A two-dimensional photonic bandgap device inhibits the propagation of light within a range of frequencies in any direction within a plane. In the device currently being investigated, the two-dimensional photonic bandgap effect is used to enhance the extraction efficiency of a light-emitting diode (LED).[18] In particular, such a device consists of an LED structure containing a periodic array of air holes. The periodic placement of the holes forms a triangular lattice and results in the presence of a photonic bandgap in the plane of the active layer. The presence of the photonic crystal inhibits the guided modes in the active layer. As light is generated in the active layer from carrier recombination, the only allowed modes for the light to couple into are the designed radiation modes. This translates to a higher flux of radiation emitted in the vertical directions. Simulations have shown the extraction efficiency of an LED using such a scheme to be more than 80-90%, compared to 10-20% in a conventional LED.

Currently, LED structures emitting at 980 nm have been grown by gas source molecular beam epitaxy and optically characterized. The fabrication process of the 2D photonic bandgap employing electron-beam lithography, reactive ion etch, and plasma-enhanced chemical vapor deposition is underway.

3.3.3 Three-Dimensional Devices: A Photonic Crystal

A three-dimensional (3D) photonic crystal requires a sophisticated geometry and an intricate arrangement of holes and rods to create a full bandgap. Unfortunately, the complex structure does not easily lend itself to fabrication at submicron length scales. Furthermore, most applications for photonic crystals require photonic bandgaps larger than 10% which, in turn, require the use of materials with a large index contrast such as in the case of GaAs and Al_xO_y or Si and SiO_2. One example of a 3D PBG structure consists essentially of two interpenetrating distributed Bragg reflectors (DBRs) composed of GaAs and Al_xO_y in which a series of holes are etched at normal incidence through the top surface of the structure. Using gas source molecular beam epitaxy, a GaAs/AlAs DBR was first deposited onto a GaAs wafer. Holographic lithography was used to expose a grating on the wafer, hence defining the position of the second DBR. In the pattern transfer procedure, the GaAs and AlAs layers beneath the photoresist lines will be removed using reactive ion etching, thus reproducing the grating in the first DBR. By regrowing the second DBR within the trenches of the grating, a periodic structure of GaAs and AlAs can be formed both normal to and parallel to the surface.

18 S. Fan, P.R. Villeneuve, J.D. Joannopoulos, and E.F. Schubert. "High Extraction Efficiency of Spontaneous Emission from Slabs of Photonic Crystals," *Phys. Rev. Lett.* 78(7): 3294-97 (1997).

After the regrowth procedure, a series of holes will be etched into the structure, and the AlAs will be oxidized to form Al_xO_y, creating a 3D photonic crystal.

3.4 Growth of Bandgap-Engineered Distributed Bragg Reflectors

Sponsors

Joint Services Electronics Program

Project Staff

Professor Leslie A. Kolodziejski, Professor Rajeev J. Ram, Dr. Gale S. Petrich, Steven G. Patterson

Semiconductor lasers are a powerful and pervasive device finding application in long-haul fiberoptic communications, local area networks, medicine, metrology, and basic research. Most commercial applications employ edge-emitting lasers. The need, however, for lasers which (1) exhibit circular beam profiles (for coupling to fibers), (2) possess the capability for forming two-dimensional arrays, (3) integrate easily with electronics, and (4) are less costly to test, has driven research on vertical cavity surface emitting lasers (VCSELs). Even more so than edge emitters, VCSELs are dependent upon growth technologies that are capable of near atomic layer precision such as that provided by molecular beam epitaxy (MBE).

A unique structural property of VCSELs is the use of distributed Bragg reflectors (DBRs) as the end mirrors of the optical cavity. Since the DBRs must not only act as optical reflectors, but also as electrical conductors, DBRs present a difficult design challenge to the successful implementation of low threshold current and voltage VCSELs. Toward this end, the current work has achieved the gas source MBE (GSMBE) growth of graded-interface DBRs utilizing $Al_{0.1}Ga_{0.9}As$ and $Al_{0.9}Ga_{0.1}As$ quarter-wave layers with a 300 Angstrom graded interface region between the layers. This is a first necessary step toward the long term goal of producing a single-mode high-power VCSEL.

Ideally, the valence band should be flat for p-type mirrors and the conduction band flat for n-type mirrors. Theoretically, this can be achieved for an arbitrary grading or doping concentration in the transition region.[19] However, the practical realities of GSMBE place sharp restrictions on what is physically realizable. In particular, the effusion cells have finite thermal mass hence limiting the maximum aluminum content gradient. Furthermore, the minimum doping density is set by the background doping density while the maximum doping density is set by such factors as the growth rate, dopant autocompensation, doping dependent diffusivities, among others.

A variety of compositional profiles and lengths were theoretically modeled to determine which would provide achievable doping densities. Reflection high-energy electron diffraction oscillations were used to experimentally determine the growth rates of GaAs and AlAs as a function of cell temperature. With this data, the necessary cell temperature profiles were then calculated. Finally, the proportional/integral/differential (PID) settings on the cell temperature controllers were adjusted to allow the grading profiles to closely match the model while minimizing over and undershoot transients. A substrate temperature of 480°C was used throughout the growth to prevent beryllium (the p-type dopant) diffusion.

To achieve acceptable reflection properties, the thickness of the graded interfacial regions must be minimized. A graded transition from GaAs to AlAs achieves the largest index contrast possible, but would result in an unacceptably wide graded region. Presently, the most practical graded transition is between $Al_{0.1}Ga_{0.9}As$ and $Al_{0.9}Ga_{0.1}As$. A further advantage of this compositional change results from the Al and Ga cells remaining open through the DBR growth process, hence eliminating the growth rate transients associated with cell shutter openings and closings. Pure AlAs should be avoided in optical devices because AlAs is easily oxidized during post-growth device processing which eventually leads to device failure.

The use of modulation doping results in equilibrium space-charge regions. When properly designed and executed, the undesired band bending in the valence or conduction bands is exactly canceled by the space charge induced electric field. The result is an order of magnitude reduction in the series resistance introduced by the DBRs.

---

19 D.I. Babic, G. H. Dohler, J. E. Bowers, and E. L. Hu, "Isotype Heterojunctions with Flat Valence or Conduction Band," *IEEE J. Quantum. Electron.* 33(12): 2195-98 (1997).

Fifteen period DBRs have been grown with 300 Angstrom $Al_{0.1}Ga_{0.9}As$ to $Al_{0.9}Ga_{0.1}As$ graded interfaces. Reflectivity and double crystal x-ray diffractometry measurements suggest that high quality graded interface DBRs have been realized. Currently, detailed doping calibrations are being done on bulk material. Upon completion, a modulation doped DBR will be realized.

Chapter 3. Epitaxial Growth and Processing of Compound Semiconductors

Academic and Research Staff

Professor Leslie A. Kolodziejski, Dr. Gale S. Petrich, Dr. Jay N. Damask

Graduate Students

Jody L. House, Elisabeth M. Koontz, Kuo-Yi Lim, Jeremy M. Milikow, Steven G. Patterson, Sean C. Warnick

Technical and Support Staff

Olga M. Arnold, Angela R. Mickunas

3.1 Introduction

The emphasis of this research program is the epitaxial growth and processing of III-V compound semiconductors. The epitaxial growth of the heterostructures is performed in the chemical beam epitaxy laboratory. The laboratory consists of two gaseous source epitaxy reactors interconnected to several smaller chambers which are used for sample introduction and *in-situ* surface analysis. Such a multichamber epitaxy system allows heterostructures to be fabricated within a continuous ultrahigh vacuum environment. The III-V gas source molecular beam epitaxy (GSMBE) reactor is equipped with (1) solid elemental sources of Ga, In, Al, Si and Be, (2) gaseous hydride sources of arsenic and phosphorus, (3) an atomic hydrogen source to remove the sample's native surface oxide prior to growth and (4) an *in situ* spectroscopic ellipsometer to characterize the epilayer during growth.

In the following sections, the status of the various III-V-based projects will be discussed. The III-V GSMBE system is utilized for (1) the development of (In,Ga)(As,P)-based optical devices for optical networks, (2) the fabrication of one-, two- and three-dimensional photonic bandgap crystals, and (3) the fabrication of bandgap-engineered distributed Bragg reflectors for vertical cavity surface emitting lasers.

3.2 Development of Semiconductor Optical Devices for All-Optical Communication Networks

Sponsors

MIT Lincoln Laboratory

U.S. Air Force - Office of Scientific Research
Grant F49620-96-1-0126

Project Staff

Professor Leslie A. Kolodziejski, Professor Erich P. Ippen, Professor Henry I. Smith, Professor James G. Fujimoto, Professor Hermann A. Haus, Dr. Mark S. Goorsky,[1] Dr. Gale S. Petrich, Dr. Katherine L. Hall, Dr. Günter Steinmeyer, Dr. Jay N. Damask, Elisabeth M. Koontz, Jeremy M. Milikow, Igor P. Bilinsky, David J. Jones, Erik R. Thoen, Thomas E. Murphy, M. Jalal Khan, Michael H. Lim, K.M. Matney,[2] Greg D. U'Ren[3]

With the next generation of all-optical networks being designed for operation at speeds of 100 Gbits/sec and higher, compact, efficient semiconductor-based optical devices are clearly in demand. In these high bit-rate networks, low-loss wavelength-selective routing devices and ultrafast (femtosecond) optical pulse sources are required.

1 Department of Material Science and Engineering, University of California, Los Angeles, California.

2 Ibid.

3 Ibid.

Waveguide-coupled Bragg-resonant filters[4] provide a compact means of achieving high-density wavelength-selective routing. The functionality of the planar version of these filters[5] is contingent upon the ability to preserve the as-fabricated rectangular-patterned Bragg gratings during the gas source molecular beam epitaxial overgrowth. Mass transport-induced degradation of the rectangular-grating profile during the epitaxial overgrowth results in the inability to selectively route the desired wavelength.[6]

Rectangular-patterned gratings, similar in dimension to those required by the Bragg-resonant filters, have been fabricated in both InP and InGaAsP. An *in-situ* low-temperature atomic hydrogen-assisted oxide removal technique has been employed to preserve the rectangular grating profile[7] as seen in Figure 1. The atomic hydrogen-assisted cleaning process is performed at 200°C, well below the temperature required to thermally desorb the native oxide from the sample's surface (~ 470°C). Thus, the overgrowth can be nucleated immediately upon arrival at the growth temperature (480°C), severely inhibiting the degradation of the grating profile via mass transport effects.

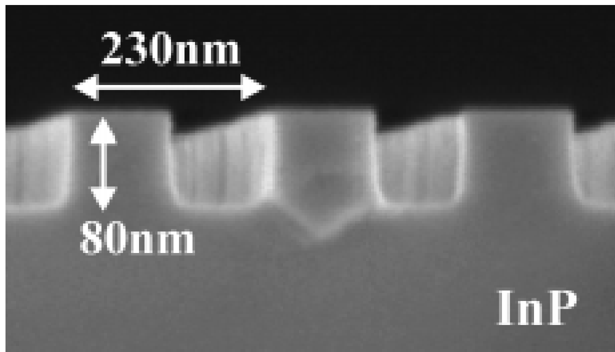

Figure 1. Scanning electron micrograph of an InP rectangular-patterned grating following the low temperature atomic hydrogen-assisted oxide removal process.

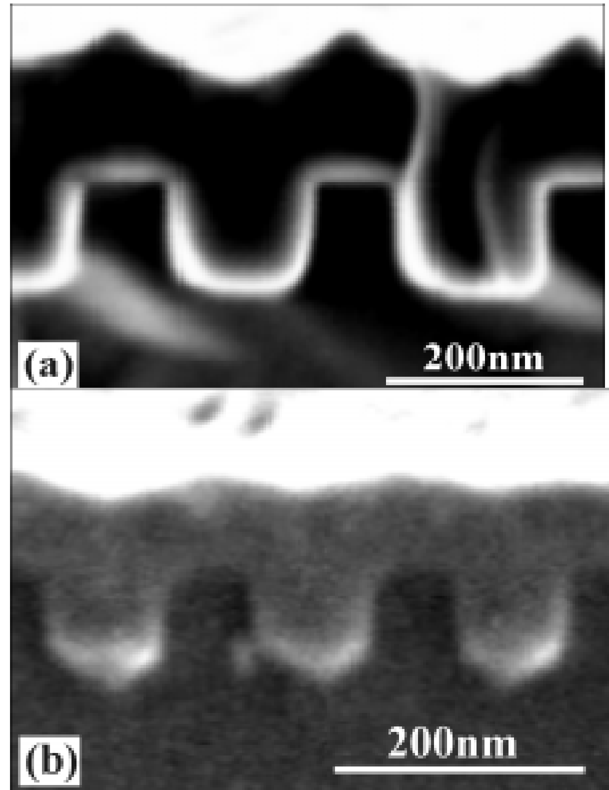

Figure 2. (a) Scanning electron micrograph of 200 nm of InGaAs deposited on a hydrogen-cleaned InP grating. (b) Scanning electron micrograph of 200 nm of InGaAs deposited on a thermally-cleaned InP grating; the as-fabricated rectangular grating shows signs of mass transport-induced profile degradation.

Figure 2 depicts a scanning electron micrograph of an overgrown hydrogen-cleaned InP grating (Figure 2a) and a thermally-cleaned InP grating (Figure 2b). The hydrogen-cleaned grating appears to be intact, while the thermally-cleaned grating has experienced profile degradation in the form of rounded grating teeth and filled-in grating trenches.

4 H.A. Haus and Y. Lai, "Narrow-Band Distributed Feedback Reflector Design," *J. Lightwave Technol.* 9(6): 754-60 (1991); H.A. Haus and Y. Lai, "Narrow-Band Optical Channel-Dropping Filter," *J. Lightwave Technol.* 10(1): 57-62 (1992).

5 J.N. Damask, "Practical Design of Side-Coupled Quarter-Wave Shifted Distributed-Bragg Resonant Filters," *J. Lightwave Technol.* 14(5): 812-21 (1996).

6 J.N. Damask, private communication.

7 E.M. Koontz, M.H. Lim, V.V. Wong, G.S. Petrich, L.A. Kolodziejski, H.I. Smith, M.S. Goorsky, and K.M. Matney, "Overgrowth of InGaAsP Materials on Rectangular-patterned Gratings Using GSMBE," *Proceedings of the Ninth International Conference on InP and Related Materials,* Hyannis, Massachusetts, May 11-15, 1997.

Triple-axis x-ray diffractometry (TAD) has been used to provide a nondestructive, high-resolution analysis of the overgrown gratings. A (004) TAD reciprocal space map of InGaAsP deposited on an InP grating is shown in Figure 3. The zeroth order satellite reflection is similar to a double crystal x-ray scan and reveals the high quality of the overgrown InGaAsP. The existence of periodic satellite fringes confirms the presence of a periodic modulation within the overgrown structure. Separation of the satellite fringes (Δ) is related to the period of the grating[8] and corresponds to an as-fabricated period of 230 nm. The vertical continuity of the satellite reflections (along q_{004}) represents the retention of the rectangular grating profile.[9] The presence of the ±2nd order satellite reflections (not expected for rectangular grating profiles having equal trench and tooth widths[10]) suggests the presence of strain within the grating region.[11] The appearance of the ±2nd order satellite reflections cannot be attributed to a mass transport-induced change in the InP grating profile from rectangular to gaussian since the higher order satellite reflections are of significant intensity.[12] (224) TAD reciprocal space maps confirm that strain is present within the grating region, and is orthorhomically distorting the crystal.[13] In other words, two of the three lattice components are strained to differing amounts, while the third lattice component is left unstrained. The magnitude of the strain is on the order of 10^{-3} and is expected to have a minimal effect on the optical characteristics of the Bragg-resonant filters.[14]

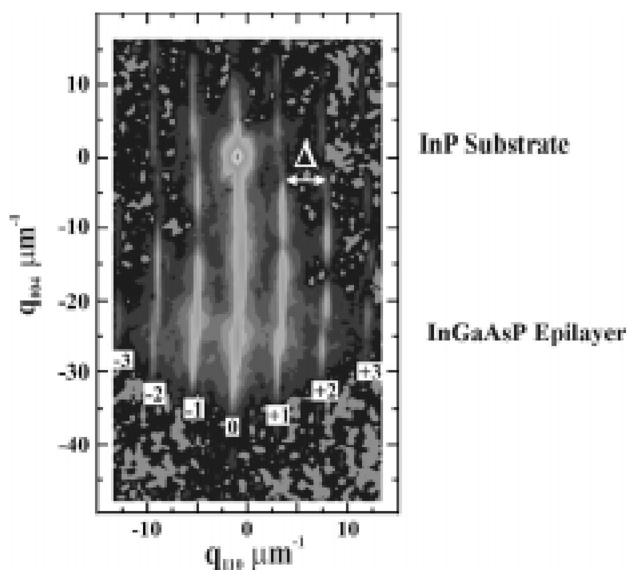

Figure 3. A (004) triple axis x-ray diffraction-generated reciprocal space map of 200 nm of $In_{0.93}Ga_{0.07}As_{0.23}P_{0.77}$ deposited on a hydrogen-cleaned InP grating.

Currently, passive modelocking is the most practical method of generating ultrashort (femtosecond) pulses in lasers. The shortest pulses achieved thus far, 6.5 fsec, are from a Ti:sapphire laser implementing a semiconductor saturable absorber mirror to initiate modelocking.[15] Ti:sapphire lasers, however, operate at a wavelength (0.75 μm) significantly below that required for efficient transmission over standard communications optical fiber (1.3 μm or 1.55 μm), upon which the all-optical communication systems are based. Various chromium-based solid-state lasers have been successfully modelocked at wavelengths within the 1.5 μm regime,[16] with the passive

8 A.T. Macrander and S.E.G. Slusky, "X-ray Diffraction from Corrugated Crystalline Surfaces and Interfaces," *Appl. Phys. Lett.* 56(5):443-45 (1990).

9 P. van der Sluis, "High Resolution X-ray Diffraction of One- and Two-dimensional Periodic Surface Gratings," *J. Phys. III France* 4: 1639-47 (1994).

10 Ibid.

11 E.M. Koontz, M.H. Lim, V.V. Wong, G.S. Petrich, L.A. Kolodziejski, H.I. Smith, K.M. Matney, G.D. U'Ren, and M.S. Goorsky, “Preservation of Rectangular-patterned InP Gratings Overgrown by Gas Source Molecular Beam Epitaxy,” *Appl. Phys. Lett.* 71(10): 1400-02 (1997).

12 G.D. U'Ren, M.S. Goorsky, E.M. Koontz, M.H. Lim, G.S. Petrich, L.A. Kolodziejski, V.V. Wong, H.I. Smith, K.M. Matney, and M. Wormington, “Analysis of Lattice Distortions in High Quality InGaAsP Epitaxial Overgrowth of Rectangular-patterned InP Gratings,” *J. Vac. Sci. Technol. B.*, forthcoming.

13 Ibid.

14 Ibid.

15 I.D. Jung, F.X. Kartner, N. Matuschek, D. Sutter, F. Morier-Genoud, U. Keller, V. Scheuer, M. Tilsch, T. Tschudi, and R. Szipocs, “Self-starting 6.5 fs Pulses from a KLM Ti:sapphire Laser,” *Proceedings of the Conference on Lasers and Electro-Optics,* (Washington, DC: Optical Society of America, 1997), 11: 35 (1997).

modelocking devices being saturable Bragg reflectors (SBRs). Also successfully modelocked (at $\lambda \sim 1.53$ μm) via an SBR is a linear erbium/ytterbium co-doped fiber laser cavity.[17] Modelocked fiber lasers offer a number of advantages over other ultrafast sources, such as their compactness and ability to be pumped with telecommunications-certified low-power laser diodes, and a wavelength of operation centered at the erbium-doped fiber gain peak of 1.55 μm.

An SBR consists of a saturable absorber (quantum wells within a half-wave layer or a bulk-like epilayer) integrated with a highly reflective mirror, a distributed Bragg reflector (DBR). By epitaxially depositing the saturable absorber directly on the mirror via gas source molecular beam epitaxy, additional fabrication steps (i.e., thinning or removing the substrate beneath the saturable absorber and using index matching epoxy to attach a saturable absorber to a commercial mirror) are avoided. In addition, by selecting the reflectivity of the DBR, the SBR can then be used as either a high reflector or an output coupler in the laser cavity.

The current SBR structures contain either two or four InGaAs quantum wells positioned 15 nm from the top of, or centered within, the InP half-wave layer. The DBR contains 22 pairs of quarter-wave AlAs/GaAs layers, resulting in a reflectivity spectrum centered at 1.55 μm. Of concern is the large lattice mismatch between the InP half-wave layer and the GaAs-based DBR. The use of a half-wave InP layer has two purposes: it does not harm the reflectivity spectrum of the DBR, yet simultaneously provides a buffer between the lattice-mismatched InP/GaAs interface and the InGaAs quantum well absorber.

The transmission spectrum from a 22-pair DBR and the photoluminescence spectrum of an SBR containing two InGaAs quantum wells centered within the InP half-wave layer are shown in Figure 4. Additional analysis performed on the SBRs include pump-probe measurements (changes in frequency and reflectivity with respect to time and wavelength) and phase change measurements (changes in the phase with respect to time and wavelength). Two SBRs, both with two InGaAs quantum wells positioned 15 nm from the top of the InP half-wave layer, have successfully modelocked a Cr^{4+}:YAG laser. Devices are currently being fabricated for implementation in erbium-doped fiber ring and sigma laser cavities as well as linear fiber cavities containing an erbium/ytterbium co-doped amplifier, all of which integrate easily with all-optical fiber networks.

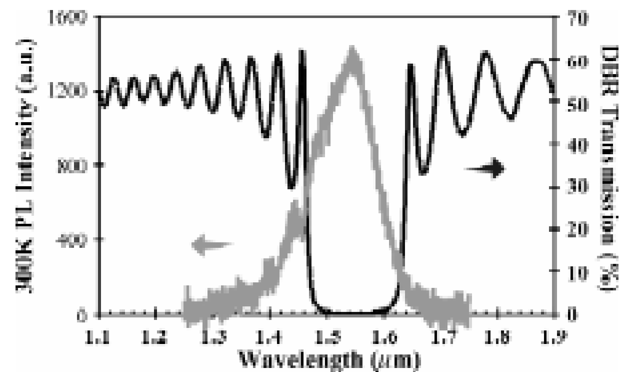

Figure 4. Transmission spectrum of a 22-pair AlAs/GaAs distributed Bragg reflector (DBR) and photoluminescence spectra of a saturable Bragg reflector consisting of the 22-pair DBR and two InGaAs quantum wells centered within an InP half-wave layer.

3.2.1 Publications

Koontz, E.M., M.H. Lim, V.V. Wong, G.S. Petrich, L.A. Kolodziejski, H.I. Smith, K.M. Matney, G.D. U'Ren, and M.S. Goorsky. "Preservation of Rectangular-patterned InP Gratings Overgrown by Gas Source Molecular Beam Epitaxy." *Appl. Phys. Lett.* 71(10): 1400-02 (1997).

Koontz, E.M., M. H. Lim, V.V. Wong G.S. Petrich, L.A. Kolodziejski, H.I. Smith, M.S. Goorsky, and K.M. Matney. "Overgrowth of InGaAsP Materials on Rectangular-patterned Gratings Using GSMBE." *IEEE Proceeedings of the Ninth International Conference on InP and Related Materials,* Hyannis, Massachusetts, May 11-15, 1997.

16 B.C. Collings, J.B. Stark, S. Tsuda, W.H. Knox, J.E. Cunningham, W.Y. Jan, R. Pathak, and K. Bergman, "Saturable Bragg Reflector Self-starting Passive Mode Locking of a Cr^{4+}:YAG Laser Pumped with a Diode-pumped Nd:YVO_4 Laser," *Opt. Lett.* 21(15): 1171-73 (1996); M.J. Hayduk, S.T. Johns, M.F. Krol, C.R. Pollock, and R.P. Leavitt, "Broadly Tunable Saturable Absorber Mode-locked Cr^{4+}:YAG Femtosecond Laser," *Proceedings of the IEEE Lasers and Electro-Optics Society Annual Meeting,* (Piscataway, N.J.: IEEE, 1996), pp. 54-55.

17 B.C. Collings, K. Bergman, S. Tsuda, and W.H. Knox, "Femtosecond Short Cavity 2.5 GHz Fiber Laser Harmonically Mode-locked by a Saturable Bragg Reflector with Low Temporal Jitter," *Proceedings of the Conference on Lasers and Electro-Optics* (Washington, D.C.: Optical Society of America, 1997); 11: 343-44 (1997).

U'Ren, G.D., M.S. Goorsky, E.M. Koontz, M.H. Lim, G.S. Petrich, L.A. Kolodziejski, V.V. Wong, H.I. Smith, K.M. Matney, and M. Wormington. "Analysis of Lattice Distortions in High Quality InGaAsP Epitaxial Overgrowth of Rectangular-patterned InP Gratings." Sixteenth North American Conference on Molecular Beam Epitaxy, Ann Arbor, Michigan, October 5-8, 1997; *J. Vac. Sci. Tech. B.* Forthcoming.

3.3 Photonic Bandgap Structures

Sponsor

National Science Foundation
Grant DMR 94-00334

Project Staff

Professor John D. Joannopoulos, Professor Leslie A. Kolodziejski, Professor Erich P. Ippen, Professor Henry I. Smith, Dr. Gale S. Petrich, Dr. Pierre R. Villeneuve, Dr. Shanhui Fan, Dr. Günter Steinmeyer, Kuo-Yi Lim, Daniel J. Ripin

This project represents the combined effort of the research groups led by Professors John D. Joannopoulos, Leslie A. Kolodziejski, Erich P. Ippen, and Henry I. Smith. Professor Joannopoulos' research group designs the structures and theoretically calculates the optical properties. Professor Kolodziejski's group fabricates various devices exhibiting photonic band structures in one-, two-, and three-dimensions using III-V compound semiconductor technologies. Professor Smith's group provides the expertise in nanoscale fabrication. Finally, the devices are optically characterized by Professor Ippen's research group. The complexity of the design, fabrication and characterization of these structures necessitates a strong interaction between the various research groups.

A photonic crystal is a periodic dielectric structure that prohibits the propagation of photons within a certain range of frequencies in all directions. This forbidden band of frequencies translates into a photonic bandgap (PBG) analogous to an electronic bandgap in a semiconductor crystal. A defect state can be introduced in the photonic bandgap when the dielectric periodicity of a photonic crystal is broken by the selective removal or addition of dielectric material. This defect results in the spatial localization of the defect mode into a volume of approximately one cubic wavelength, yielding a low modal volume, high-quality factor resonant microcavity. The realization of such a microcavity holds the promise of vastly enhancing the performance of optoelectronic devices through its effect on spontaneous emission.

3.3.1 One-Dimensional Photonic Bandgap Devices: Monorail and Air-Bridge Microcavities

The one-dimensional photonic bandgap devices that are being investigated at MIT are referred to as monorail and air-bridge microcavity devices. In the monorail microcavity, the photonic crystal consists of a GaAs waveguide with an array of holes etched through the waveguide. The holes are spaced periodically and a defect is created by introducing additional separation in the middle of the array. The photonic crystal resides on a layer of aluminum oxide (Al_xO_y) which has a much lower refractive index than GaAs (n = 1.61 versus n = 3.3). In the air-bridge microcavity, the photonic crystal is suspended in air (n = 1.0), resulting in a higher index contrast between the crystal and its surroundings. The devices are designed to operate at the technologically important wavelength of 1.55 μm. Consequently, the photonic crystal has a width of 0.5 μm and a thickness of 0.2 μm. The hole diameter, separation, and defect width are 0.2 μm, 0.4 μm, and 0.6 μm respectively. Both the monorail and air-bridge microcavities have waveguides coupled into and out of the devices to facilitate the optical characterization of these devices.

The fabrication process for the devices utilize a heterostructure of $GaAs/Al_{0.9}Ga_{0.1}As$ grown by gas source molecular beam epitaxy. Subsequently, a series of plasma-enhanced chemical vapor deposition, electron-beam lithography, reactive ion etch, photolithography and wet etch processing steps are employed to fabricate the final devices. The samples are then thinned from 400 μm to 150 μm before a final cleave is performed to create mirror-smooth facets at the waveguide ends for optical coupling. Both the monorail and air-bridge microcavity structures have been successfully fabricated and are currently being characterized. Figure 5 shows a scanning electron micrograph of a completed one-dimensional photonic bandgap device.

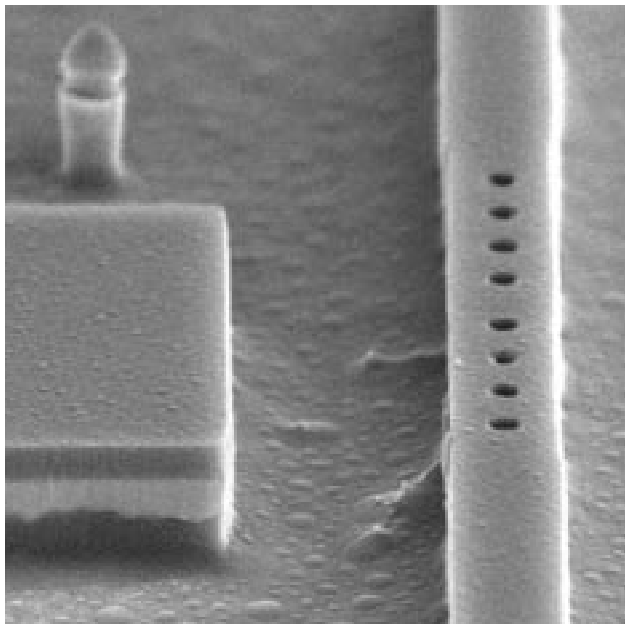

Figure 5. A micrograph of a PBG monorail structure with a GaAs waveguide. The width and thickness of the bridge are 0.5 μm and 0.2 μm, respectively. The diameter and separation of the holes are 0.4 μm and 0.6 μm, respec-tively.

The one-dimensional photonic crystal results in the confinement of light of a particular wavelength along the direction of the waveguide. At the same time, the light is also confined in the other two directions by total internal reflection. The wavelength of light being confined in the microcavity is determined by the dimensions and separation of the holes in the photonic crystal. The combination of the high-index contrast of the system and the presence of the photonic crystal results in a high-Q, low-modal volume microcavity. Such a microcavity can effectively alter the spontaneous emission rate of an active region located in the microcavity.

3.3.2 Two-Dimensional Photonic Bandgap Device: Enhancing the Extraction Efficiency of a Light Emitting Diode

A two-dimensional photonic bandgap device inhibits the propagation of light within a range of frequencies in any direction within a plane. In the device currently being investigated, the two-dimensional photonic bandgap effect is used to enhance the extraction efficiency of a light-emitting diode (LED).[18] In particular, such a device consists of an LED structure containing a periodic array of air holes. The periodic placement of the holes forms a triangular lattice and results in the presence of a photonic bandgap in the plane of the active layer. The presence of the photonic crystal inhibits the guided modes in the active layer. As light is generated in the active layer from carrier recombination, the only allowed modes for the light to couple into are the designed radiation modes. This translates to a higher flux of radiation emitted in the vertical directions. Simulations have shown the extraction efficiency of an LED using such a scheme to be more than 80-90%, compared to 10-20% in a conventional LED.

Currently, LED structures emitting at 980 nm have been grown by gas source molecular beam epitaxy and optically characterized. The fabrication process of the 2D photonic bandgap employing electron-beam lithography, reactive ion etch, and plasma-enhanced chemical vapor deposition is underway.

3.3.3 Three-Dimensional Devices: A Photonic Crystal

A three-dimensional (3D) photonic crystal requires a sophisticated geometry and an intricate arrangement of holes and rods to create a full bandgap. Unfortunately, the complex structure does not easily lend itself to fabrication at submicron length scales. Furthermore, most applications for photonic crystals require photonic bandgaps larger than 10% which, in turn, require the use of materials with a large index contrast such as in the case of GaAs and Al_xO_y or Si and SiO_2. One example of a 3D PBG structure consists essentially of two interpenetrating distributed Bragg reflectors (DBRs) composed of GaAs and Al_xO_y in which a series of holes are etched at normal incidence through the top surface of the structure. Using gas source molecular beam epitaxy, a GaAs/AlAs DBR was first deposited onto a GaAs wafer. Holographic lithography was used to expose a grating on the wafer, hence defining the position of the second DBR. In the pattern transfer procedure, the GaAs and AlAs layers beneath the photoresist lines will be removed using reactive ion etching, thus reproducing the grating in the first DBR. By regrowing the second DBR within the trenches of the grating, a periodic structure of GaAs and AlAs can be formed both normal to and parallel to the surface.

18 S. Fan, P.R. Villeneuve, J.D. Joannopoulos, and E.F. Schubert. "High Extraction Efficiency of Spontaneous Emission from Slabs of Photonic Crystals," *Phys. Rev. Lett.* 78(7): 3294-97 (1997).

After the regrowth procedure, a series of holes will be etched into the structure, and the AlAs will be oxidized to form Al_xO_y, creating a 3D photonic crystal.

3.4 Growth of Bandgap-Engineered Distributed Bragg Reflectors

Sponsors

Joint Services Electronics Program

Project Staff

Professor Leslie A. Kolodziejski, Professor Rajeev J. Ram, Dr. Gale S. Petrich, Steven G. Patterson

Semiconductor lasers are a powerful and pervasive device finding application in long-haul fiberoptic communications, local area networks, medicine, metrology, and basic research. Most commercial applications employ edge-emitting lasers. The need, however, for lasers which (1) exhibit circular beam profiles (for coupling to fibers), (2) possess the capability for forming two-dimensional arrays, (3) integrate easily with electronics, and (4) are less costly to test, has driven research on vertical cavity surface emitting lasers (VCSELs). Even more so than edge emitters, VCSELs are dependent upon growth technologies that are capable of near atomic layer precision such as that provided by molecular beam epitaxy (MBE).

A unique structural property of VCSELs is the use of distributed Bragg reflectors (DBRs) as the end mirrors of the optical cavity. Since the DBRs must not only act as optical reflectors, but also as electrical conductors, DBRs present a difficult design challenge to the successful implementation of low threshold current and voltage VCSELs. Toward this end, the current work has achieved the gas source MBE (GSMBE) growth of graded-interface DBRs utilizing $Al_{0.1}Ga_{0.9}As$ and $Al_{0.9}Ga_{0.1}As$ quarter-wave layers with a 300 Angstrom graded interface region between the layers. This is a first necessary step toward the long term goal of producing a single-mode high-power VCSEL.

Ideally, the valence band should be flat for p-type mirrors and the conduction band flat for n-type mirrors. Theoretically, this can be achieved for an arbitrary grading or doping concentration in the transition region.[19] However, the practical realities of GSMBE place sharp restrictions on what is physically realizable. In particular, the effusion cells have finite thermal mass hence limiting the maximum aluminum content gradient. Furthermore, the minimum doping density is set by the background doping density while the maximum doping density is set by such factors as the growth rate, dopant autocompensation, doping dependent diffusivities, among others.

A variety of compositional profiles and lengths were theoretically modeled to determine which would provide achievable doping densities. Reflection high-energy electron diffraction oscillations were used to experimentally determine the growth rates of GaAs and AlAs as a function of cell temperature. With this data, the necessary cell temperature profiles were then calculated. Finally, the proportional/integral/differential (PID) settings on the cell temperature controllers were adjusted to allow the grading profiles to closely match the model while minimizing over and undershoot transients. A substrate temperature of 480°C was used throughout the growth to prevent beryllium (the p-type dopant) diffusion.

To achieve acceptable reflection properties, the thickness of the graded interfacial regions must be minimized. A graded transition from GaAs to AlAs achieves the largest index contrast possible, but would result in an unacceptably wide graded region. Presently, the most practical graded transition is between $Al_{0.1}Ga_{0.9}As$ and $Al_{0.9}Ga_{0.1}As$. A further advantage of this compositional change results from the Al and Ga cells remaining open through the DBR growth process, hence eliminating the growth rate transients associated with cell shutter openings and closings. Pure AlAs should be avoided in optical devices because AlAs is easily oxidized during post-growth device processing which eventually leads to device failure.

The use of modulation doping results in equilibrium space-charge regions. When properly designed and executed, the undesired band bending in the valence or conduction bands is exactly canceled by the space charge induced electric field. The result is an order of magnitude reduction in the series resistance introduced by the DBRs.

19 D.I. Babic, G. H. Dohler, J. E. Bowers, and E. L. Hu, “Isotype Heterojunctions with Flat Valence or Conduction Band,” *IEEE J. Quantum. Electron.* 33(12): 2195-98 (1997).

Fifteen period DBRs have been grown with 300 Angstrom $Al_{0.1}Ga_{0.9}As$ to $Al_{0.9}Ga_{0.1}As$ graded interfaces. Reflectivity and double crystal x-ray diffractometry measurements suggest that high quality graded interface DBRs have been realized. Currently, detailed doping calibrations are being done on bulk material. Upon completion, a modulation doped DBR will be realized.